Effects of Large Energetic Vortices on Axial-Flow Hydrokinetic Turbines

B. Gunawan[1], V.S. Neary[1] C. Hill[2] and L.P. Chamorro[2]

[1]Energy-Water-Ecosystems Engineering, Wind and Water Power Technologies, Environmental Sciences Division, Oak Ridge National Laboratory, One Bethel Valley Road, P.O. Box 2008, MS-6036, Oak Ridge, TN 37831; PH (865) 241-5622; FAX (865) 576-3989; email: gunawanb@ornl.gov
[2]St. Anthony Falls Laboratory, College of Science & Engineering, University of Minnesota, Minneapolis, MN 55414.

ABSTRACT

Large scale coherent motions around marine and hydrokinetic (MHK) machines can significantly increase the structural loading and affect the overall performance of the machines. Characterization of the approach turbulence and their impact on the instantaneous response of MHK devices is essential for improving their design and performance. This preliminary study investigates the effect of turbulence and dominant energetic coherent structures induced by a vertical cylinder on the structural load and energy production in a model MHK turbine. Results show that the power generated by the turbine is significantly reduced by the presence of the cylinder. This reduction depends on the distance from the cylinder and the level of turbulence around the rotor area.

INTRODUCTION

Hydraulic and natural instream structures increase turbulence levels and introduce large scale coherent structures to the flow around MHK machines. These features affect the structural loading on the machine and its annual energy production . ADV measurements at the centerline of the energy extraction plane, or axial-flow turbine hub elevation, provide high resolution measurements that are crucial for obtaining accurate estimation of hydrodynamic loading and energy production. They also support the development of turbulent water inflow models, like the TurbSim model used for simulating turbulent wind flows (Jonkman 2009).

Vortex shedding generated by bluff bodies has been quantified in great detail using laser Doppler velocimetry (LDV) and particle image velocimetry (PIV) in laboratory channels. While these methods provide unique insights about the complexity of a flow, they are not practical for measurement around large or full scale MHK machines in the field. In this study three synchronized acoustic Doppler velocimeters (ADVs) are deployed along the transverse direction in the wake of a cylinder positioned upstream of a 1:10 axial flow turbine model to characterize the vortex shedding introduced into the turbine inflow. The effects of the vortex shedding and turbulence on structural loading and energy production are investigated.

MEASUREMENT DETAILS

The research described herein was completed in the St. Anthony Falls Laboratory (SAFL) Main Channel facility. The SAFL Main Channel is approximately 2.8m wide, 1.8m deep, and 85m long with a maximum flow discharge of approximately 8.5m^3/s. This facility uses the Mississippi River as its untreated water source and can operate continuously and indefinitely. Water enters the channel through a mechanical headgate to the Mississippi River, passes through a series of flow straighteners and eddy-break grid, flows through the Main Channel and over a mechanical tailgate at the end of the channel, returning to the Mississippi River. The discharge rate is monitored using a Massa ultrasonic range sensor mounted upstream of the sharp-crested weir tailgate. For these experiments, the discharge (Q), depth (h) and bulk velocity (U_∞) were 1.265m^3/s, 1.15m and 0.4m/s respectively. The SAFL Main Channel Data Acquisition (DAQ) Carriage, capable of completing longitudinal, lateral, and vertical travel within 1mm accuracy, was utilized to position instruments for data acquisition (Figure 1a).

A cylinder PVC pipe with a diameter (D_p) of 0.115m was used to induce specific and energetic coherent motions upstream of a hydrokinetic turbine scale model with a rotor diameter (D_t) of 0.5m. The diameter size was chosen for another study, currently in progress, for investigating the effect of vortex shedding to the turbine power time series. The pipe was located with its center positioned at x/D_p = 7.5, 10, and 15 upstream of the turbine rotor plane, with x being the distance between turbine rotor and center of the pipe. This corresponds to approximately 0.86m, 1.15m, and 1.73m upstream of the turbine rotor plane, respectively. For each experiment, velocity was measured using three synchronized Nortek Vectrino II ADVs at 200Hz for 600s. The ADVs were fixed at 0.5m at upstream of the turbine. The ADVs separating distances in the transverse direction, between the left and the center and the center and the right ADVs, were set to $D_t/2$=0.25m. Throughout the rest of this paper, the right, center and left ADVs (when looking downstream) will be called ADV1, ADV2 and ADV3 respectively (Fig. 1b). The velocity data obtained were post-processed to calculate relevant parameters using the algorithm described in Gunawan et al. (2011).

DISCUSSION OF RESULTS

The mean velocities and turbulence intensities for the ADV measurements are presented in Table 1. Longitudinal velocity magnitude decreases when the cylinder is present. The decrease is more pronounced when the ADVs are closer to the cylinder, for example, the longitudinal velocity magnitude for the cylinder 7.5*Dp* case is 36% less than the magnitude for the cylinder 10*Dp* case. Turbulence intensities for all velocity components increase when the cylinder is introduced. The turbulence intensities increase significantly at position 2 because of the low longitudinal velocity magnitude at the location.

Alternations between the right and left Karman vortices in the wake of the cylinder can be clearly observed from the transverse velocity time series at position 2 (Fig. 2.). Positive values in the graph indicate that the velocity direction is towards the left bank of the Main Channel, and vice versa. The vortex shedding frequency

(f_K), defined here as the frequency of the shedding in one side of the cylinder (Naudascher & Rockwell 2005), can be roughly estimated from Fig. 2. by inverting the period between two subsequent positive (or negative) peaks of the ADV2 transverse velocity time series. The periods between two subsequent same sign peaks are approximately 1.4s, hence, f_K is approximately 0.71Hz.

Transverse velocity spectral energy densities (SED) of the approach flow and at downstream of the cylinder for the three ADVs are shown in Figure 3. The approach flow (no obstacle case) shows a short energy $f^{5/3}$ cascade, characteristic of the inertial subrange region. For the cylinder cases, the Karman Vortex shedding frequency is clearly seen with a peak at around 0.71Hz in the S_{vv} plot (Fig. 3b.). It appears to be the most energetic coherent motion over the full spectrum of scales present in the flow. The observed f_K, 0.71 Hz, is the same as the theoretical f_K value calculated based on Reynolds and Strouhal numbers. Fig. 3b. also shows that TKE in all frequency increases when the cylinder is present. Furthermore, TKE levels decrease with distance from the cylinder as expected.

Hydrodynamic forces and theoretical power density, after applying Reynold's decomposition, can be calculated using the following equations (Neary and Gunawan 2012),

$$F_D = \frac{1}{2}\rho\, C_D \left(1 + \frac{\overline{u'^2}}{\overline{u^2}}\right) \bar{u}^2$$

$$P = \frac{1}{2}\rho C_D \; A \left(1 + 3\,\frac{\overline{u'^2}}{\overline{u^2}} + \frac{\overline{u'^3}}{\overline{u^3}}\right) \bar{u}^3$$

where F_D is hydrodynamic loading, ρ is water density, C_D is net drag coefficient P is turbine mean power and A is the energy extraction plane. The effect of the cylinder to the hydrodynamic load acting on the energy extraction plane and the generated power is evaluated using the mean of the velocities measured at the three ADV locations. The load and power decrease when the cylinder is present (Fig. 4.). The load and power slowly recover as the distance from the cylinder increases.

CONCLUSIONS

Velocity and turbulence in the wake of a cylinder were measured using three synchronized ADVs to investigate the effect of turbulence and large scale coherent structures around marine and hydrokinetic (MHK) machines. It was demonstrated that the ADVs can provide high resolution measurement suitable for quantifying the vortex shedding generated by the cylinder. Preliminary observations suggest that hydrodynamic load and power decrease with the cylinder presence. The load and power slowly recover as the distance from the cylinder increases.

ACKNOWLEDGEMENT

The author thanks the Office of Energy Efficiency and Renewable Energy (EERE) of the Department of Energy (DOE) who provided funding under DOE Contract DE-AC05-00OR22725.

REFERENCES

Gunawan, B., Neary, V.S. and McNutt, J.R. (2011) "ORNL ADV post-processing guide and MATLAB algorithms for MHK site flow and turbulence analysis." *ORNL/TML-2011/338*, September 2011.

Jonkman, B.J. (2009) "TurbSim user's guide, version 1.50." *Technical Report NREL/TP-500-46198.*

Naudascher, E. and Rockwell, D. (2005) *Flow induced vibrations: an engineering guide*, Dover Publications.

Neary, V.S. and Gunawan, B. (2012) "Effects of turbulence on hydrodynamic forces and power." *ORNL TML*, submitted to PTS.

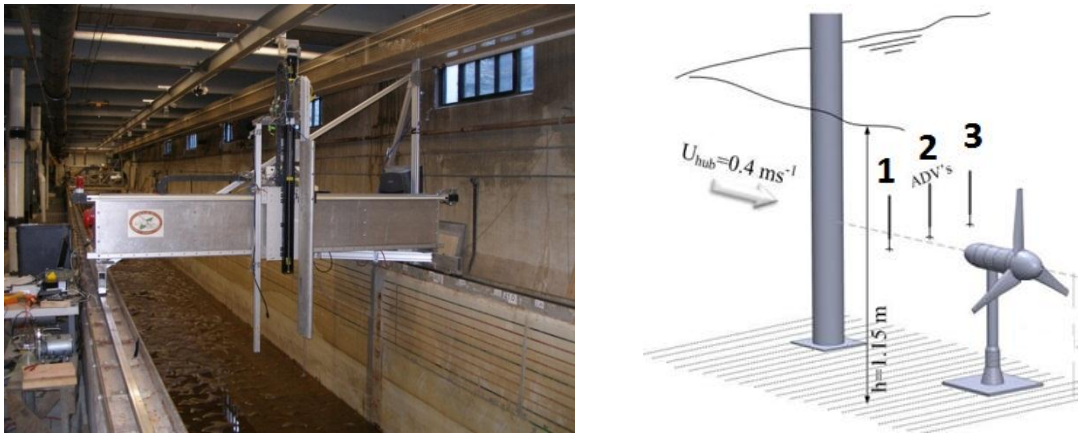

Fig. 1. Schematic of the experiments(a) and SAFL Main Channel and DAQ carriage(b).

	ADV no.	$\overline{u}$ (m/s)	$\frac{\sqrt{u'^2}}{\overline{u}}$ (%)	$\overline{v}$ (m/s)	$\frac{\sqrt{v'^2}}{\overline{u}}$ (%)	$\overline{w}$ (m/s)	$\frac{\sqrt{w'^2}}{\overline{u}}$ (%)
No obstacle	1	0.46	6.4	-0.01	5.4	-0.01	3.4
	2	0.47	5.6	-0.01	5.0	-0.02	3.1
	3	0.48	5.1	0.02	4.7	-0.01	2.9
Cylinder7.5Dp	1	0.48	8.7	0.00	6.4	-0.02	4.2
	2	0.16	190.6	-0.01	177.5	0.04	56.9
	3	0.48	7.6	0.01	6. 6	-0.01	4.3
Cylinder10Dp	1	0.45	6.3	-0.01	5.9	-0.02	3.4
	2	0.27	35.3	-0.01	48.4	0.03	22.2
	3	0.45	8.3	0.02	6.9	-0.02	3.9
Cylinder15Dp	1	0.44	9.8	-0.01	9.7	-0.02	4.8
	2	0.36	19.2	-0.01	22.6	0.04	13.1
	3	0.45	10. 7	0.01	10.7	-0.02	5.1

Table 1. Mean velocities and turbulence intensities for no obstacle and cylinder cases.

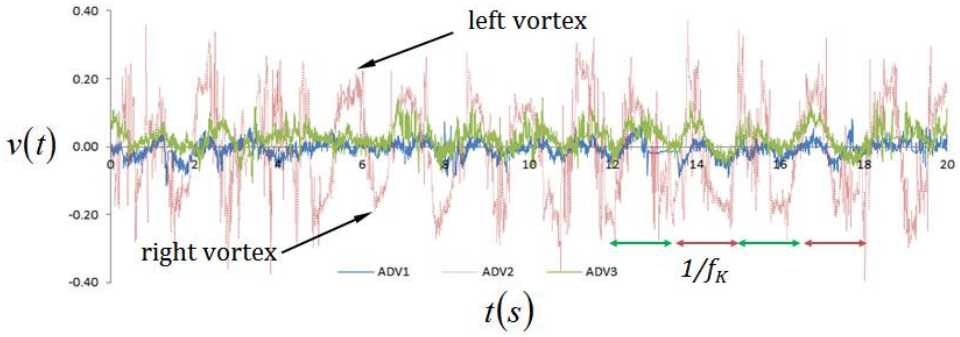

Fig. 2. Lateral velocity timeseries for the cylinder 10Dp case.

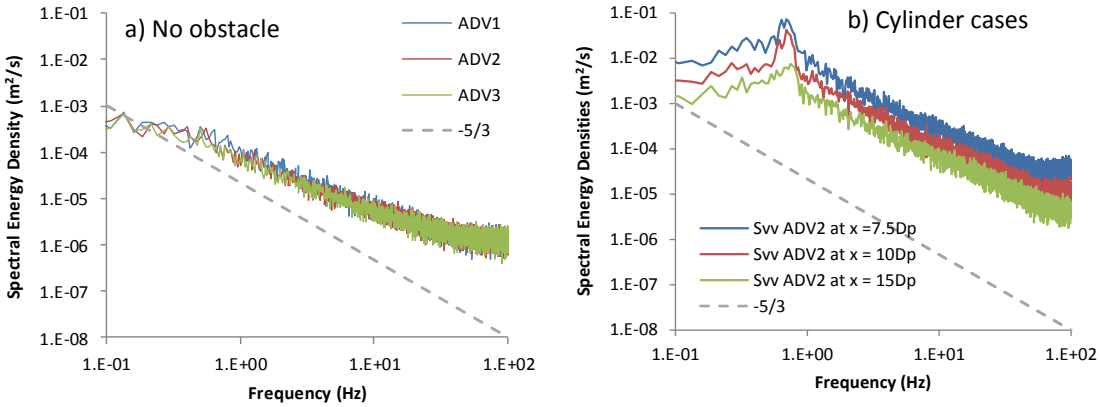

Fig. 3. Spectral energy densities of the transverse velocity component (S_{vv}) for (a) no obstacle case and (b) cylinder cases.

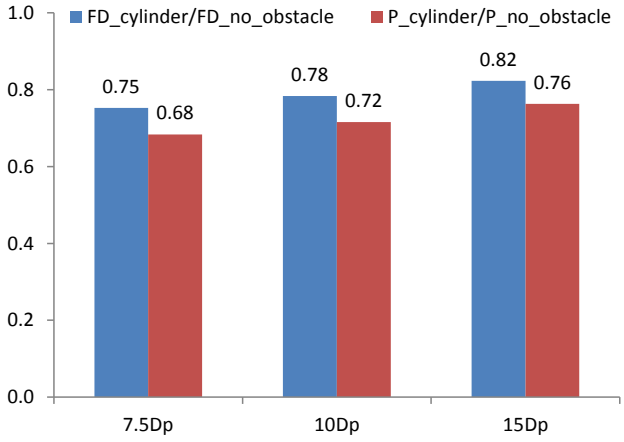

Fig. 4. Reduction of load and power with the presence of the cylinder.